SANDIA REPORT
SAND2018-3901
Unlimited Release
Printed April, 2018

Copper Hugoniot measurements to 2.8 TPa on Z

Michael D. Furnish[1] and Tom Haill[2]

[1]Dynamical Material Properties Department 1646
[2]HEDP Theory Department 1641

Prepared by
Sandia National Laboratories
Albuquerque, New Mexico 87185 and Livermore, California 94550

Sandia National Laboratories is a multimission laboratory managed and operated by National Technology and Engineering Solutions of Sandia LLC, a wholly owned subsidiary of Honeywell International Inc. for the U.S. Department of Energy's National Nuclear Security Administration under contract DE-NA0003525.

Issued by Sandia National Laboratories, operated for the United States Department of Energy by Sandia Corporation.

SAND2018-xxxx
Unlimited Release
Printed March, 2018

Copper Hugoniot measurements to 2.8 TPa on Z

Michael D. Furnish[1] and Tom Haill[2]

[1]Dynamical Material Properties Department 1646
[2]HEDP Theory Department 1641

Sandia National Laboratories
P.O. Box 5800
Albuquerque NM 87185-1195

Abstract

We conducted three Hugoniot and release experiments on copper on the Z machine at Hugoniot stress levels of 0.34 and 2.6 TPa, using two-layer copper/aluminum impactors travelling at 8 and 27 km/s and Z-quartz windows. Velocity histories were recorded for 4 samples of different thicknesses and 5 locations on the flyer plate (3 and 4 for the first two experiments). On-sample measurements provided Hugoniot points (via transit time) and partial release states (via Z-quartz wavespeed). Fabrication of the impactor required thick plating and several diamond-machining steps. The lower-pressure test was planned as a 2.5 TPa test, but a failure on the Z machine degraded its performance; however, these results corroborated earlier Cu data in the same stress region. The second test suffered from significant flyer plate bowing, but the third did not. The Hugoniot data are compared with the Al'tshuler/Nellis nuclear-driven data, other data from Z and elsewhere, and representative Sesame models.

Acknowledgments

As with any program relying on ride-along slots for Z experiments, we owe thanks to the program sponsoring those experiments (here, DOE Campaign 2), and to the many people required to assemble and execute a set of shots on Z. Included in this are Jim Williams and Lynn Twyeffort (designers), the Target Fab group, Marcus Knudson (a go-to for various parts of the preparation), and Christian Arrington and his team (responsible for the difficult copper plating). Sandia National Laboratories is a multimission laboratory managed and operated by National Technology and Engineering Solutions of Sandia LLC, a wholly owned subsidiary of Honeywell International Inc., for the U.S. Department of Energy's National Nuclear Security Administration under contract DE-NA0003525.

Table of Contents

Figures

Tables

Copper Hugoniot measurements to 2.8 TPa on Z

1.0 Introduction and Background

Copper is an fcc metal generally assumed to remain in this phase until melting, although there have been suggestions of transition to bct (body-centered tetragonal) under some conditions [e.g. Neogi and Mitra, 2017]. This makes it a good candidate for being a reference material for shock wave studies. As well, its density (8.94 gm/cc) and good electrical conductivity make it a choice material for driver plates in pulsed-power EOS experiments. Therefore it is interesting to explore its Hugoniot and release properties under a wide range of conditions.

The present study is designed to determine the Hugoniot of copper in the range 2.5 – 3.0 TPa (25 – 30 MBar). A stretch goal is to obtain one or both of a partial release state or the Hugoniot sound speed of this material.

Representative earlier Hugoniot points are plotted together with predictions by Sesame EOS 3325 in Fig. 1.1.

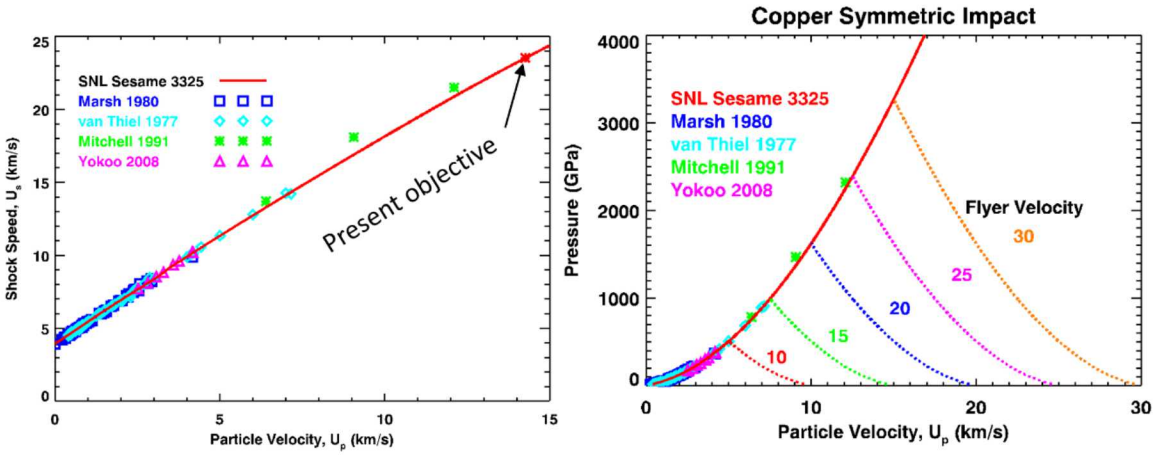

Figure 1.1. Hugoniot of copper.

2.0 Experimental Configuration

2.1 General description

The present study uses a single-sided stripline design as shown in Fig. 2.1. The flyer panel is composite, with 200 mm of plated copper backed by 800 mm of aluminum. The Z machine current, denoted by I, gives rise to Lorentz forces that launch the flyer to the left and the relatively massive tungsten cathode to the right. This allows (1) a symmetric copper → copper impact, and (2) higher impact velocities than could be achieved with a simple copper flyer. The desired impact velocity was 25 – 30 km/s. VISAR (Barker and Hollenbach, 1972; Dolan, 2006) was used for velocimetry measurements. The use of Z-cut α-quartz windows (Knudson and Desjarlais, 2009a,b) allow the VISAR measurement of shock velocity, giving additional information about the partially released state produced when the shock front passes from the copper into the quartz window. The VISAR probes were bare-fiber probes set back ~ 1 mm from the windows.

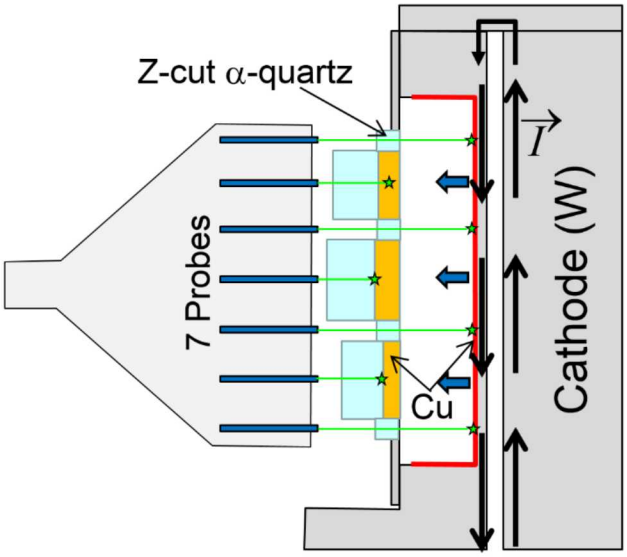

Figure 2.1. Copper experiment configuration. Stars show points where velocity is monitored by VISAR. Copper samples are yellow; quartz windows are cyan.

With this shot design it is in principle possible to measure not only the Hugoniot, but also a partial release state or a Hugoniot sound speed. Consider the wave interaction diagram in Fig. 2.2. The wavespeed in the copper sample (deduced from the observed arrival time on the waveform, the sample thickness, and the relative impact time), combined with the impact velocity and the sample density, yields the Hugoniot state. The observed plateau velocity (Fig. 1.3 center and right, denoted as V_{obs}), combined with the known quartz Hugoniot, gives the pressure and particle velocity of the copper partial release state. Combined with the Hugoniot point it is possible to calculate the density of the partial release state and the wavespeed of the transition.

With multiple sample thicknesses, we may be able to measure the Hugoniot sound speed from the thickness dependence of the arrival times of the release on the waveform.

However, for sample thicknesses > 0.5 mm, the release may overtake the initial shock wave before arriving at the sample/window interface.

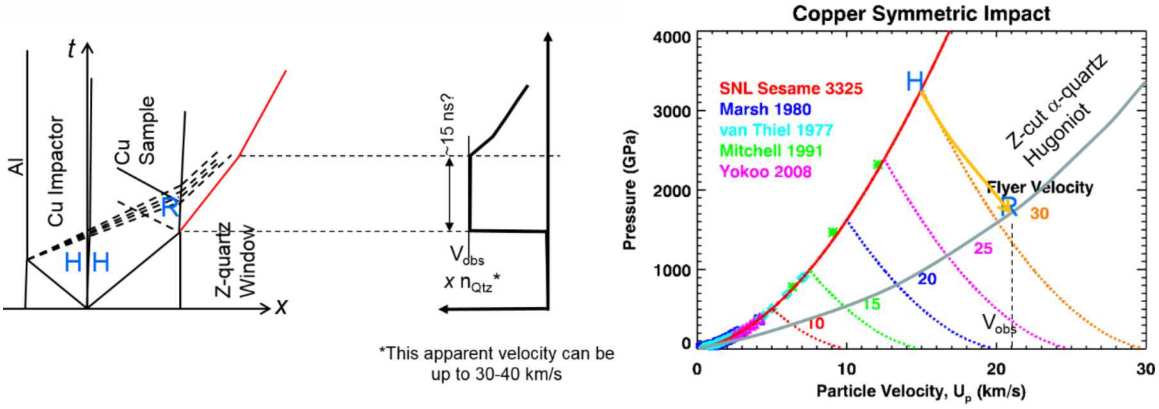

Figure 2.2. Wave interactions in copper experiment. (Left) Time vs. position diagram and expected waveform. Dashed lines are release fan. (Right) Pressure vs. particle velocity diagram, showing partial release to quartz Hugoniot.

2.2. Shot design features refined by modeling

This shot design is based on the earlier design used for shots Z2006 (Fig. 2.3) and Z2027 (Lemke et al, 2011). Shot Z2006 reached a record velocity of 28 km/s with an aluminum/copper composite flyer. Z2027 used an aluminum flyer and reached a record velocity of 40 km/s. Shock data were not obtained for the Ta sample on either shot, perhaps due to the 90° bend of the optical fiber in the diagnostic housing. The present hardware is therefore updated based on recent best practices.

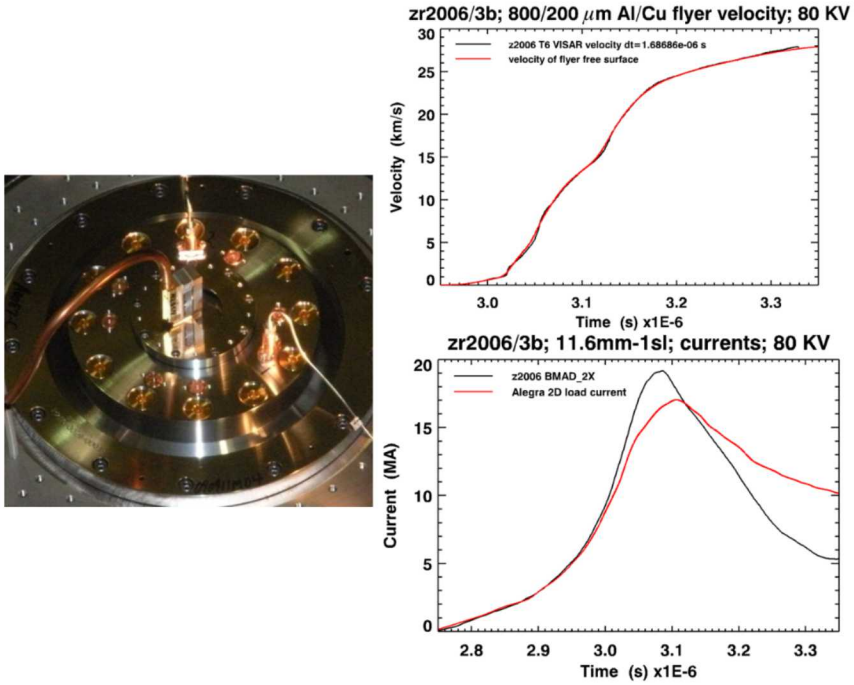

Figure 2.3. Z shot 2006, October, 2009: hardware, flyer velocity, drive current.

Large-scale 3D MHD simulations on Cielo show plasma generation near the base of the anode panel (Fig. 2.4). This is not seen in lower-resolution simulations, and may contribute to previously unexplained load current losses as well as posing a risk to diagnostics. This plasma traverses the anode-cathode (A-K) gap to the cathode and is swept upward along the gap.

Adding a bevel near the base of the anode panel (panel with the samples) helps to mitigate plasma generation up to 15 ns.

These simulations used an 87 mm diameter, 66 mm tall mesh with 335.6 M elements, 1.006 B element edges. They ran on 2400 nodes (38,400 cores) for 6 days. The mesh resolution at the core of the mesh was 40 microns.

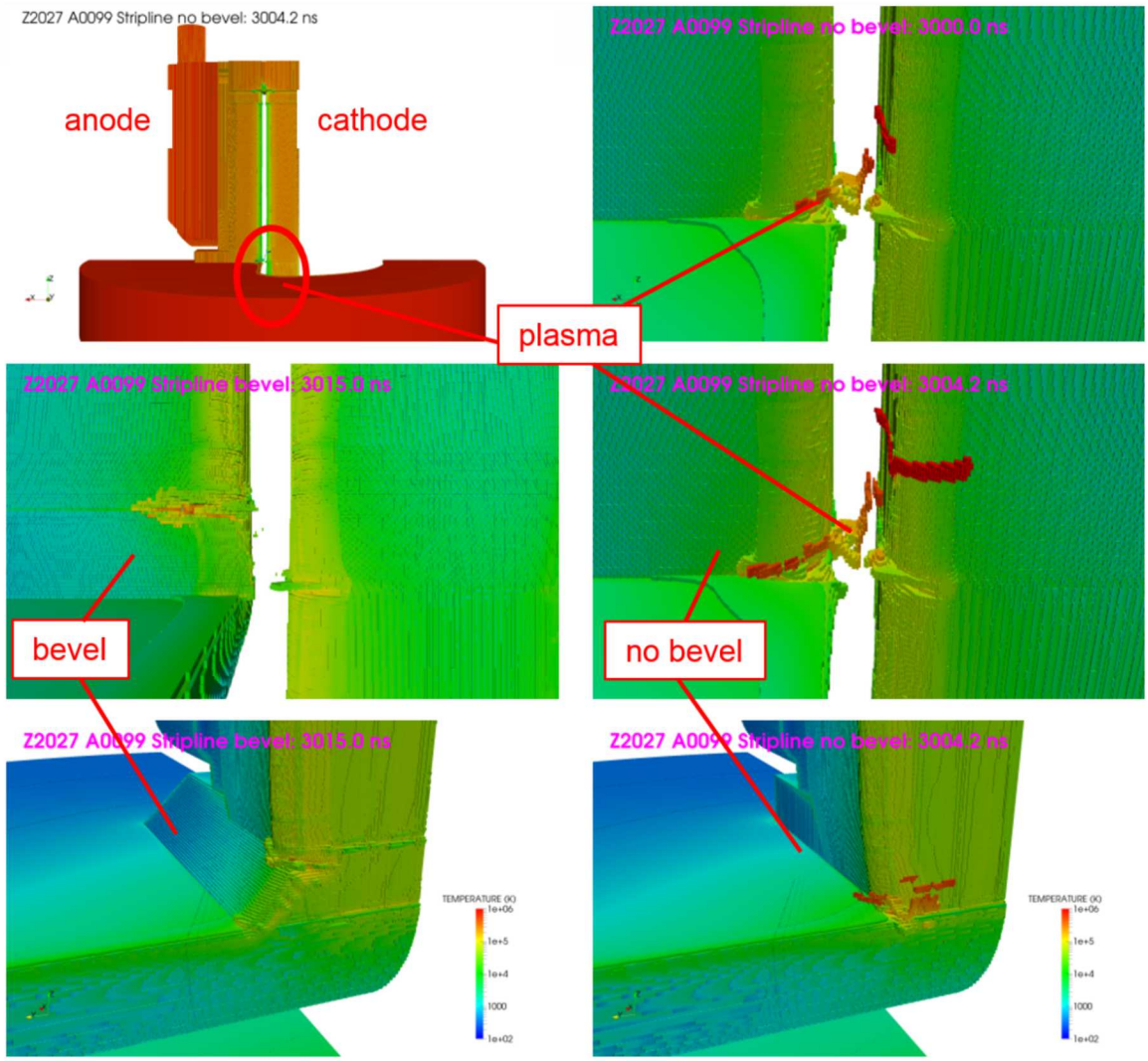

Figure 2.4. Cielo MHD calculations showing plasma generation with and without anode bevel

Another area of the shot design refined by modeling is the Z pulse shape. New Bertha models began with the configuration from Z2006 and sought to smooth the foot of the current pulse. This was to reduce the energy delivered to heat the panel and possibly melt the flyer plate. An unfold of the load current (Lemke method) was used to estimate former losses for comparison with the new design. The results are shown in Fig. 2.5 (note that these are dated due to data loss from a hard drive crash).

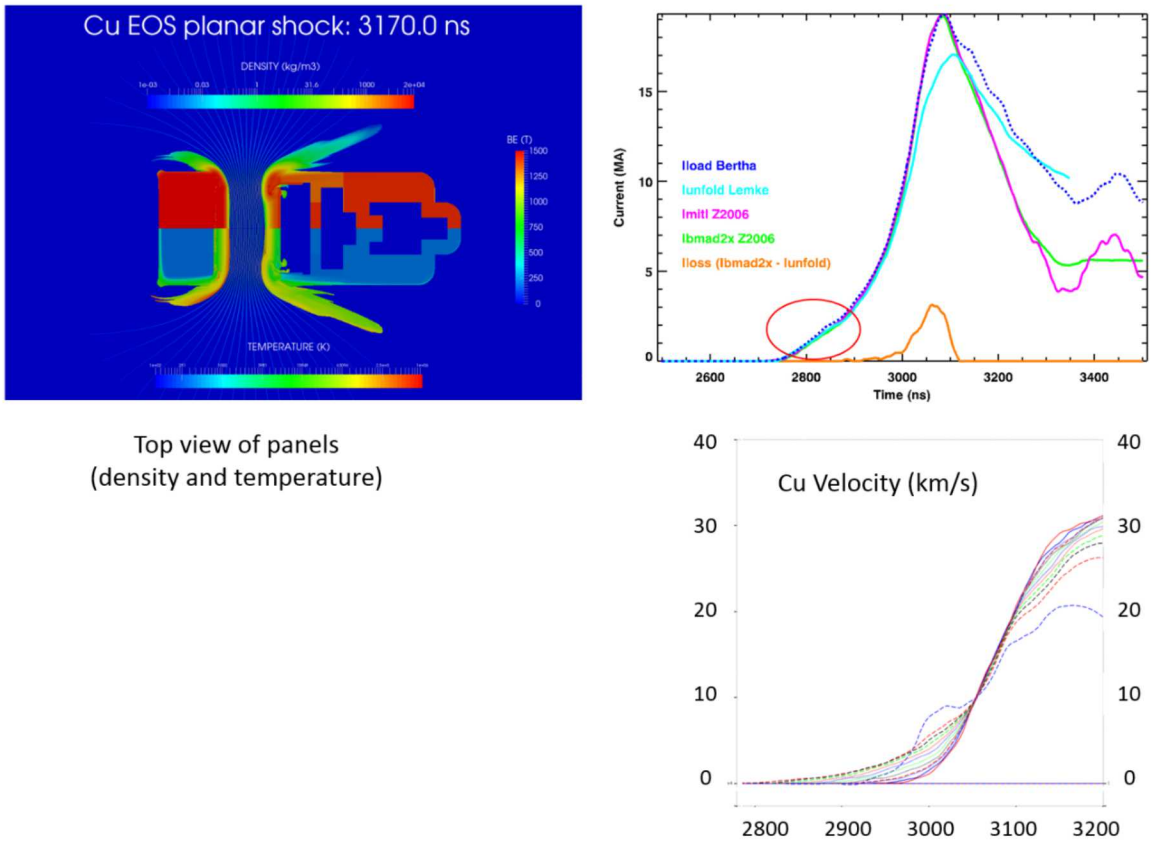

Figure 2.5. Pulse shape and resultant Cu velocity (depth dependent) and density and temperature of panel components.

2.3. Fabrication

The composite plate is a fabrication challenge. An earlier plating capability used in Z2006 (October, 2009) was no longer available, so a new capability had to be located or developed.

Consider this part (Fig. 2.6). It is an aluminum piece with 800 mm of aluminum and 200 mm of copper in the flyer plate portion. The new design has a single rectangular slot. The toe of the stripline has flairs to reduce inductance and plasma generation and increase peak current. The slot is ~ 6 mm deep, chosen to give a flight distance of 4 – 5 mm after allowing for samples projecting into the slot.

This part is fabricated in a 5-step process:

1. Machine rough (32 μinch) with 4.2" Al flyer
2. Diamond machine slot base and sides
3. Plate copper to ~380 μm (43 – 72 hours; 66% success)
4. Machine flyer to just over final thickness
5. Diamond machine copper, Al back and base

The most difficult step is the thick-plating of the copper with proper adhesion to the diamond-machined aluminum.

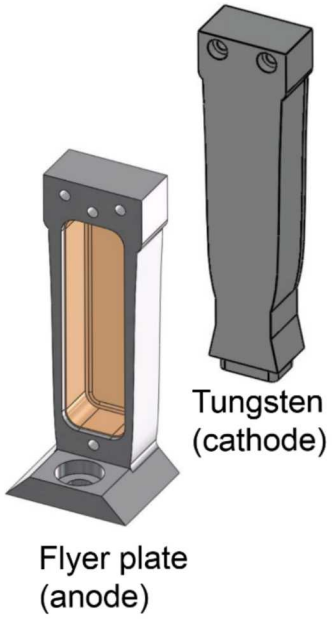

Figure 2.6. Anode panel, with layered impactor

The plating process (step 3 above) took 43 – 72 hours for the first test device and initial batch of 3 devices (Table 2.1), of which two achieved full adhesion of the copper to the aluminum.

Table 2.1. Parameters for plating of first anode panels. Sides and bottom refer to Cu thickness

	First test device	Device 01	Device 02	Device 03
Sides	355 μm	600 μm	645 μm	690 μm
Bottom	350 μm	514 μm	515 μm	464 μm
Plating time	45.8 hr	42.8 hr	59.1 hr	71.2 hr
Average current	254 mA	203 mA	169 mA	171 mA
Average thickness	355 μm	579 μm	612 μm	634 μm
Images after plating				

The final assemblies are shown in Fig. 2.7. The probe holder eliminates the 90° bend used on the 2009 shots. The bevel on the anode base shaped to reduce plasma production is clear in the middle image. The cross-section to the left illustrates the 3 sample thicknesses, chosen as approximately 0.2, 0.5 and 0.3 mm (top to bottom).

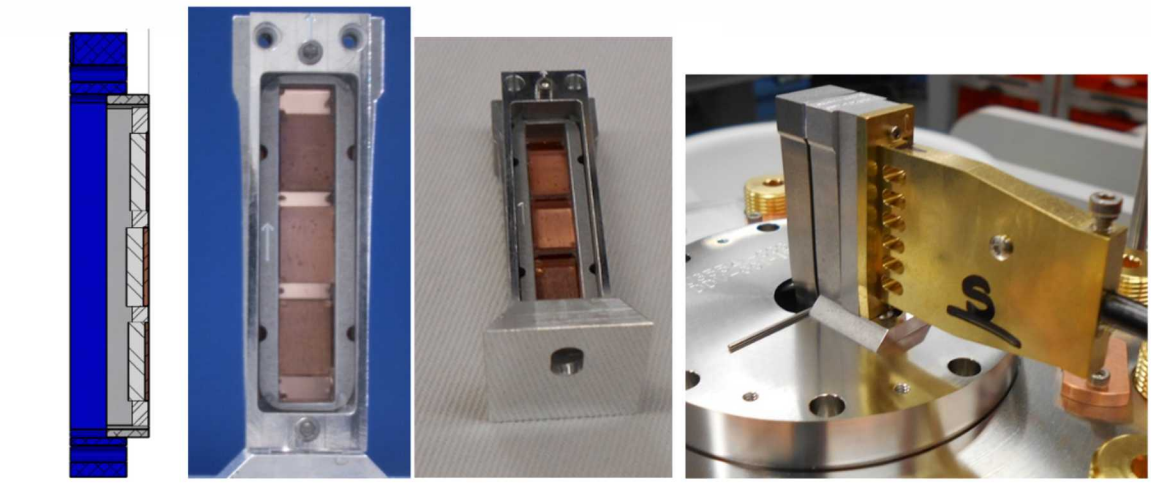

Figure 2.7. Assembled anode panel (left 3 images) and overall assembly (right).

3.0 Results

3.1 Shot Z2837 – A Zinger

The first attempt at this experiment, conducted on July 27, 2015, suffered from a Z machine short which diverted more than half of the current away from the target. Termed "zingers," these phenomena involve the development of an unexpected electrical pathway in the Magnetically Insulated Transmission Line (MITL) portion of Z.

The velocimetry results for this test are summarized in Fig. 3.1.

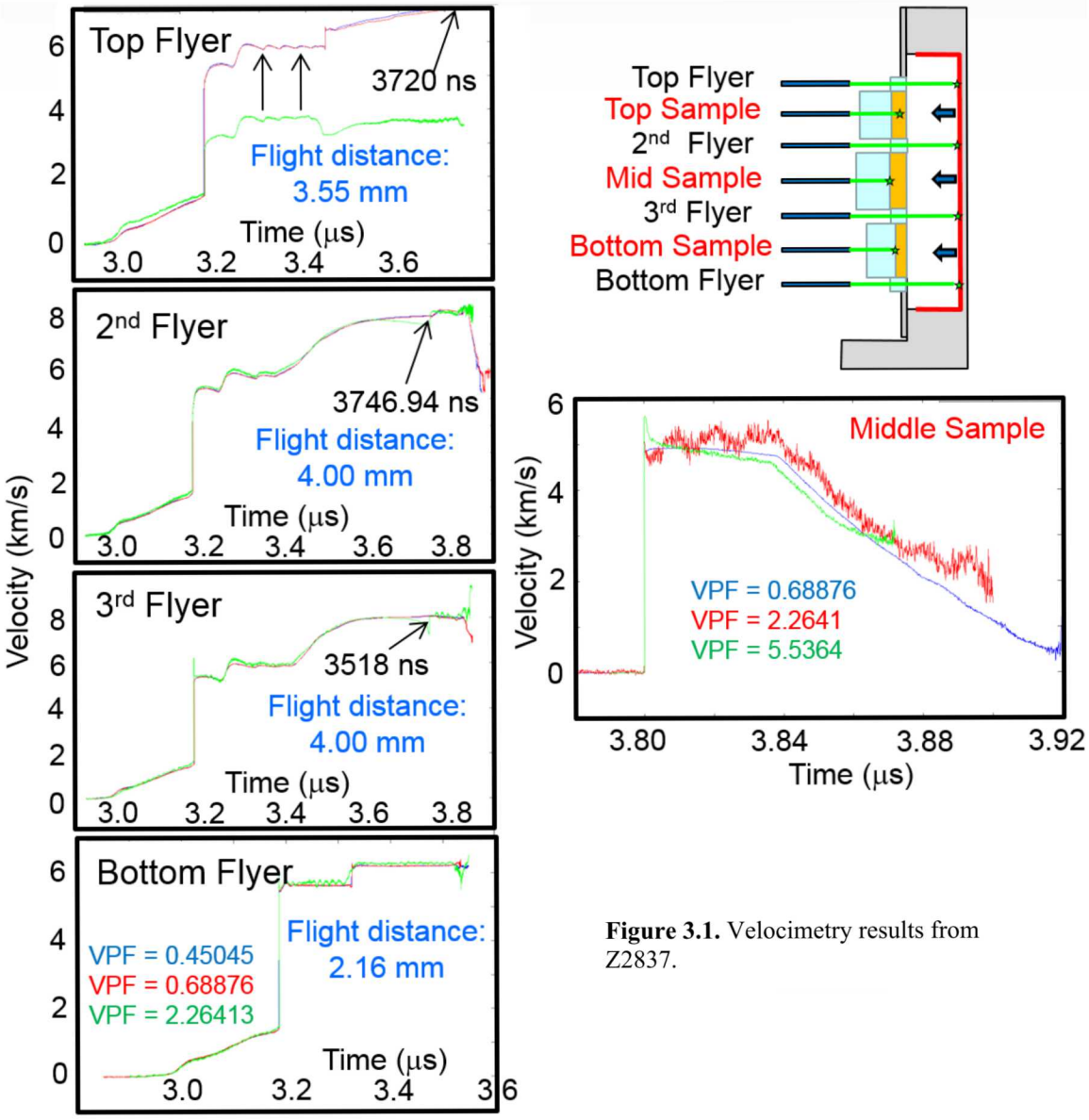

Figure 3.1. Velocimetry results from Z2837.

The flyer velocity recorded by the second and third flyer-viewing VISAR probes was 8.05 km/s instead of the planned 25- 30 km/s. That these two probes recorded the velocity through impact is supported by the fact that the velocity to apparent impact

integrates to 4.00 mm, which is the nominal flight distance. The top and bottom flyer-viewing VISAR probes did not show impact time, possibly due to flyer deformation. Those velocities integrated to 3.55 and 2.16 mm, respectively. All flyer-viewing probes showed an abrupt jump in the flyer velocity of ~4 km/s at an intermediate point in the launch, reflecting an unplanned pulse-shape due to the zinger. As well, for each waveform, the three VISAR channels (fringe sensitivities of 0.45045, 0.68876 and 2.26413 km/s/fringe) gave consistent results.

The middle sample velocimetry showed an expected waveform, with the three VISAR channels again giving generally consistent results. This was the only sample we attempted to interpret because the waveforms for the two adjacent flyer-viewing spots were clean (as noted above). It was possible to deduce the impact time on the sample, and therefore the wavespeed and the Hugoniot state. The resulting Hugoniot point is shown in Fig. 3.2 juxtaposed on selected earlier data and the Sesame 3320 and 3325 models.

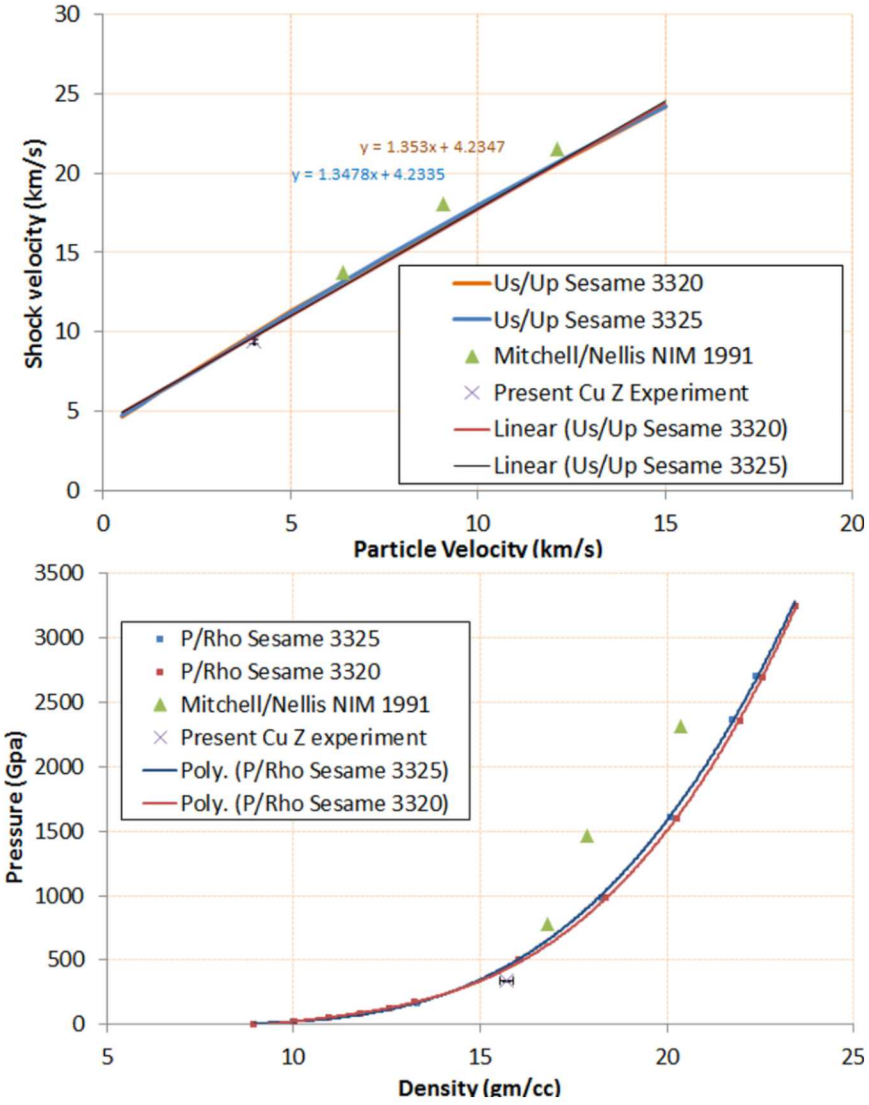

Figure 3.2. Hugoniot results for Cu from Z2837 (1 point)

3.2 Shot Z2875 – Distorted flyer plate

A new experiment was built with the other panel that showed good adhesion of the copper to the aluminum. Nevertheless, this panel had a small area which had a scuffed appearance (Fig. 3.3), affecting the area of the impactor directly under the top copper sample.

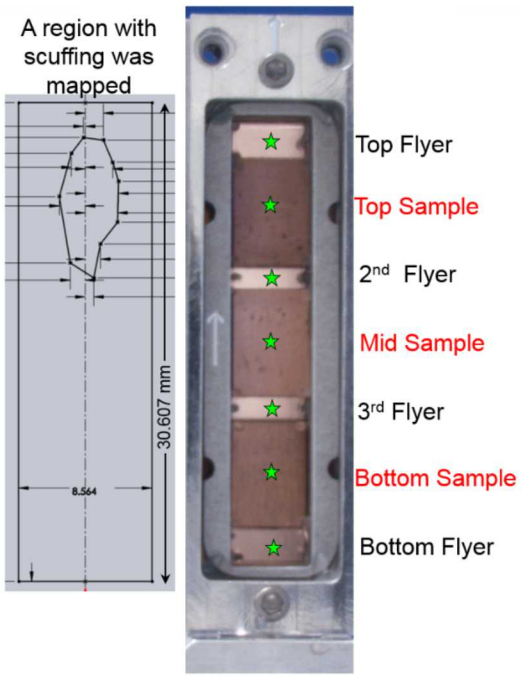

Figure 3.3. Flyer plate for second shot. Stars are points monitored by VISAR.

The velocimetry results are summarized in Fig. 3.3. The impact velocity of 27 km/s was achieved. As with the first shot, the top flyer-viewing spot did not give usable data, but the other spots did. The flyer impact times, corrected for slight differences in flight distance, are shown in Fig. 3.4. The bottom two flyer measurements were very close in time (~0.5 ns apart), while the second preceded those by nearly 8 ns. The top flyer impact was not measured, but is suspected to be 5 – 10 ns before the second flyer impact.

The flyer plate shape upon impact is deduced from the observed impact times for the flyer-viewing probe measurements, with results shown in Fig. 3.5. The impact times under the copper samples are determined by interpolating the flyer-viewing measurements (corrected for flight distance changes). Whether this interpolation is best done as linear, quadratic or other is debatable; the differences at least give an idea of the uncertainty in the result.

The resulting Hugoniot points are shown in Fig. 3.6. That the uncertainties from the points deduced from the two samples do not overlap is troublesome. This may be due to a more complicated flyer shape leading to impact. Alternatively, the thicker sample may experience release overtake. However, that thicker sample has a higher measured shock velocity than the thinner, which is the reverse of what would be expected.

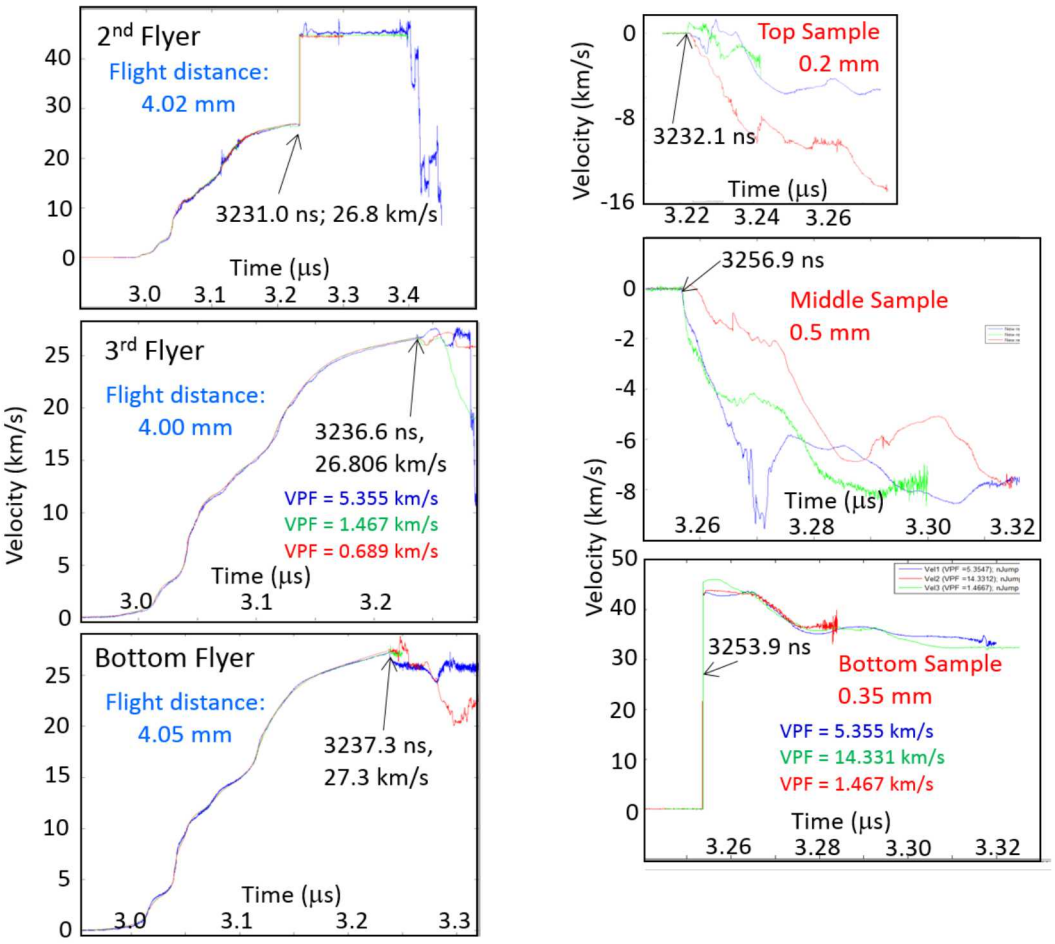

Figure 3.4. Summary of velocimetry for Z2875. Fringe jumps are added for the bottom sample, but not for the top or middle. Thicknesses are approximate.

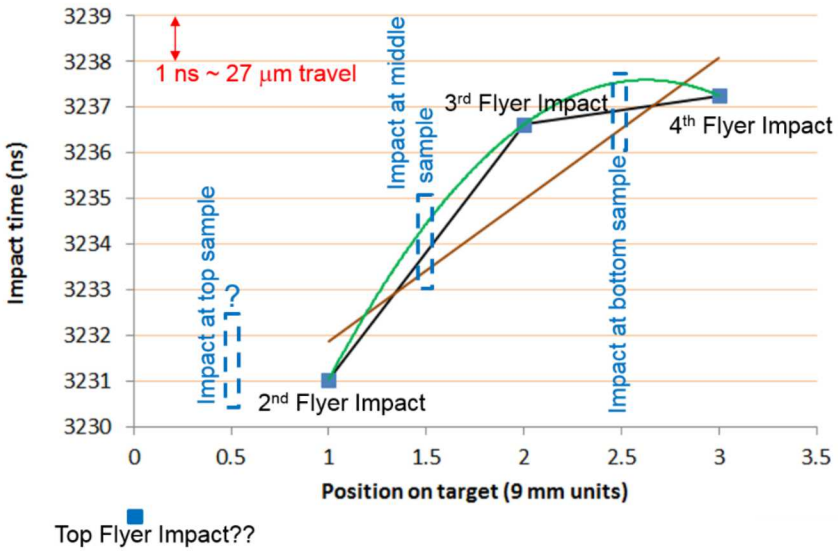

Figure 3.5. Impact time versus position for shot Z2875. Inferred impact times for the respective samples are shown as blue dashed rectangles. Horizontal axis unit (9 mm) is center:center distance for Cu samples.

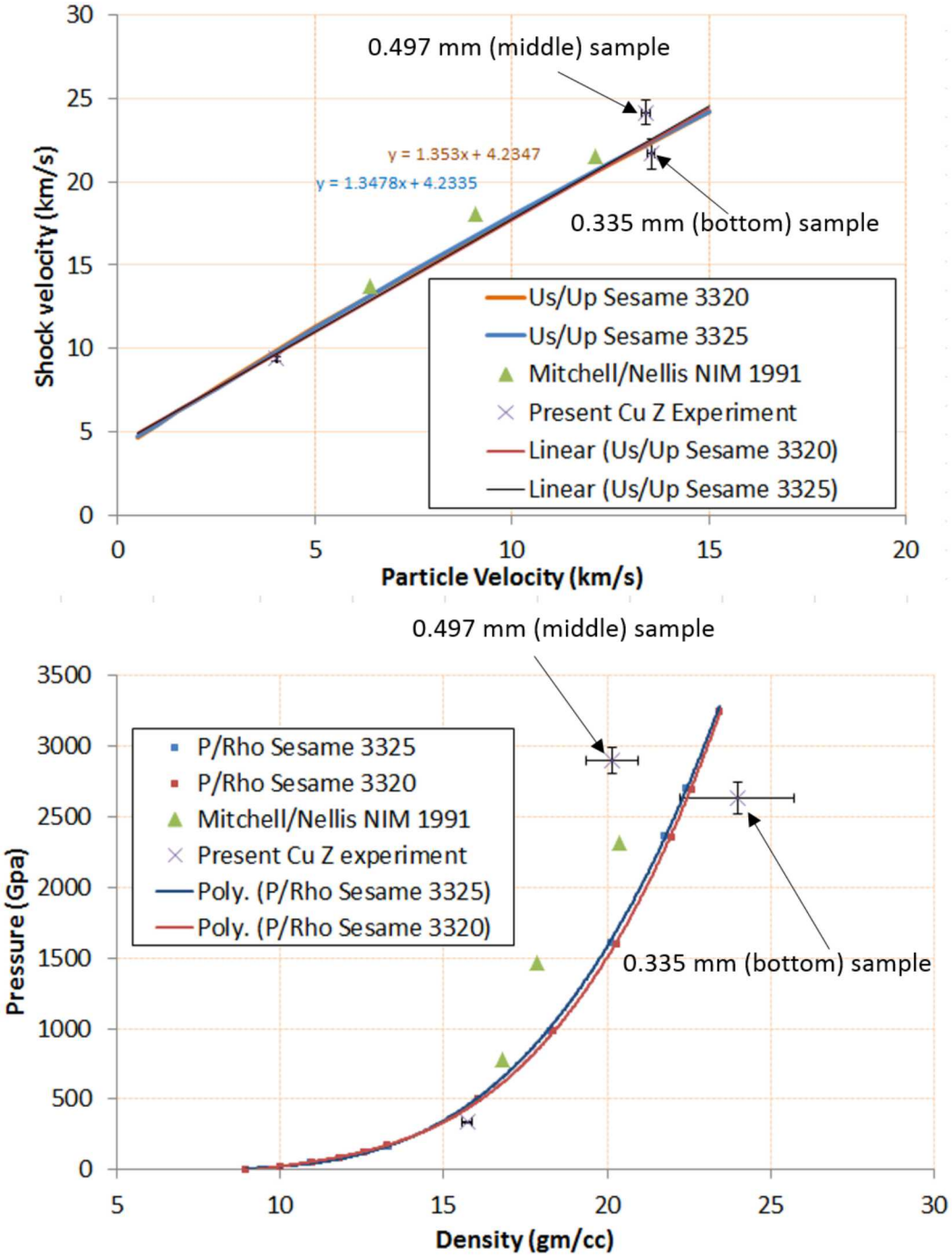

Figure 3.6. Hugoniot results for Cu from Z2837 (1 point) and Z2875 (2 points)

It is worth asking how sensitive these Hugoniot points are to the inferred impact time. Fig. 3.7 gives an idea of this sensitivity, with perturbations in steps of 1 ns applied to the assumed impact time on the two bottom Cu samples in Z2875. It is clear that a 1 ns step causes a significant change in the Hugoniot point, in particular, for the thinner (~0.395 mm) sample.

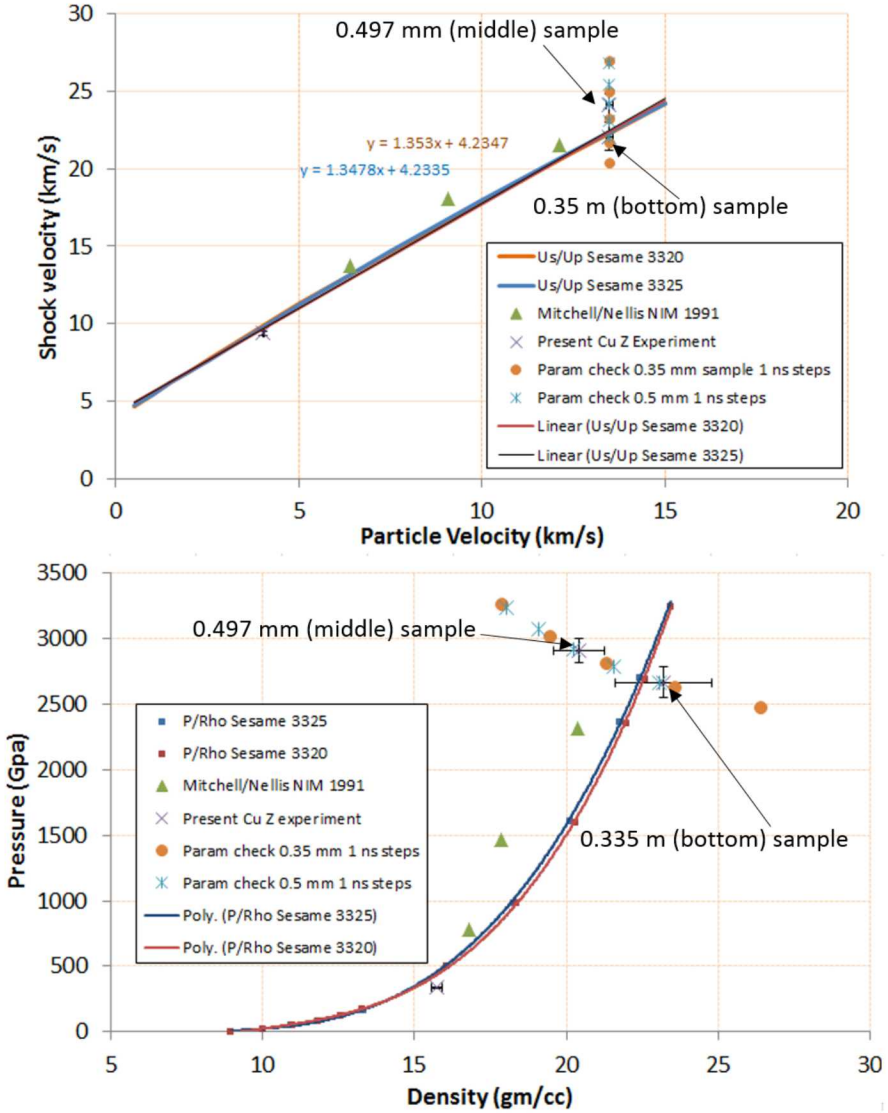

Figure 3.7. Effect on Hugoniot point of perturbing the impact time on Z2875 samples by increments of 1 ns.

Previous studies (e.g. Lemke et al, 2003) do show bowing of the flyer plates, but primarily in the horizontal direction (referenced to the present test geometry). Our interest is in the orthogonal (vertical) direction.

3.3 Shot Z3106 – More samples and measurements

Based on the lessons of Z2875, a third shot was prepared (including a new anode panel) with four copper samples and five flyer-viewing probes (Fig. 3.8). The flyer plate was accelerated smoothly to 27 km/s over a 4 mm flight distance. As with the earlier shots, the top flyer plate measurement terminated early. The flyer plate measurements are summarized in Fig. 3.9.

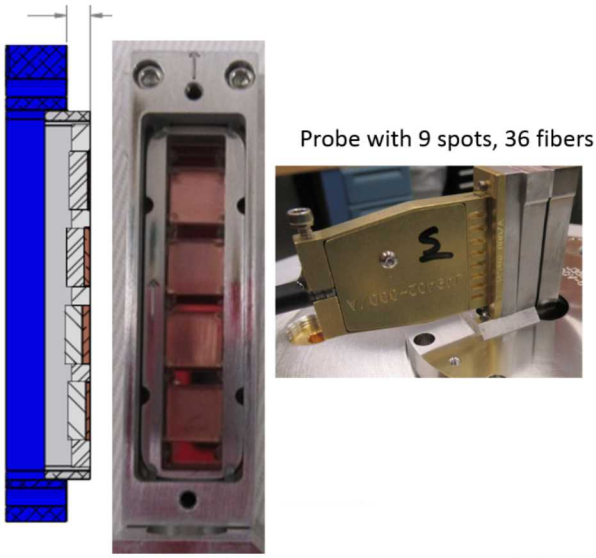

Figure 3.8. Sample cross-section and map photograph of Z3106 apparatus

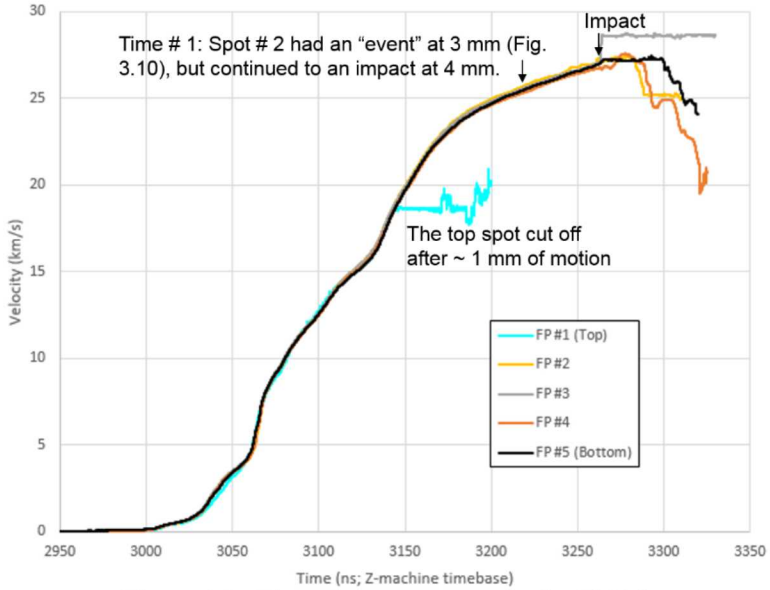

Figure 3.9. Flyer plate measurements for Z3106.

The second spot from the top showed a discontinuity after propagating 3 mm (i.e. at 3222 ns; see Fig. 3.10). It is unclear how much this might affect the nature of the impact under the adjacent copper samples (the two top samples).

Turning to the samples, let us look at all waveforms for evidence of rarefaction overtake. Fig. 3.11 shows these, together with a position vs. time diagram showing an incipient rarefaction-overtake wave interaction. Thicker samples will show more overtake effect (manifested by decreasing wave amplitude and speed). For Z2875, it is ambiguous whether the thickest sample (0.5079 mm) showed overtake, while neither of the thinner samples did. For Z3106, the two thicker samples are likely showing some rarefaction overtake.

The Hugoniot plots with these new data are shown in Fig. 3.12. The most credible datum is the 0.338 mm point (no overtake and not adjacent to the anomalous launch).

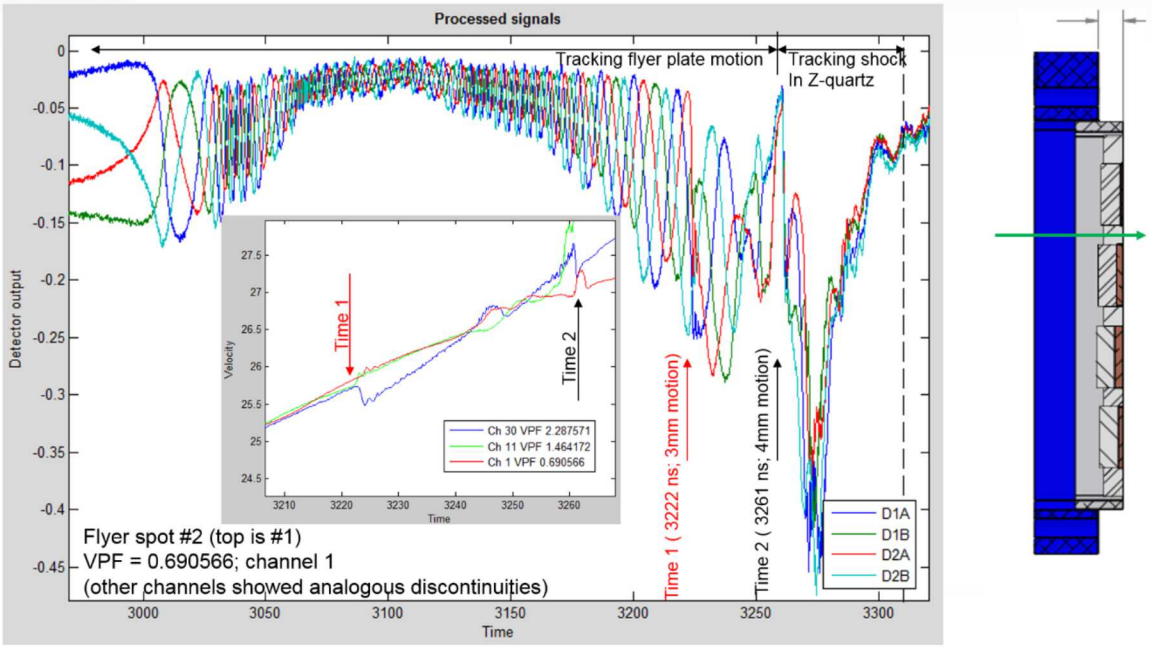

Figure 3.10. Sample fringe record, velocity detail, and locator section for discontinuity on Flyer # 2 spot.

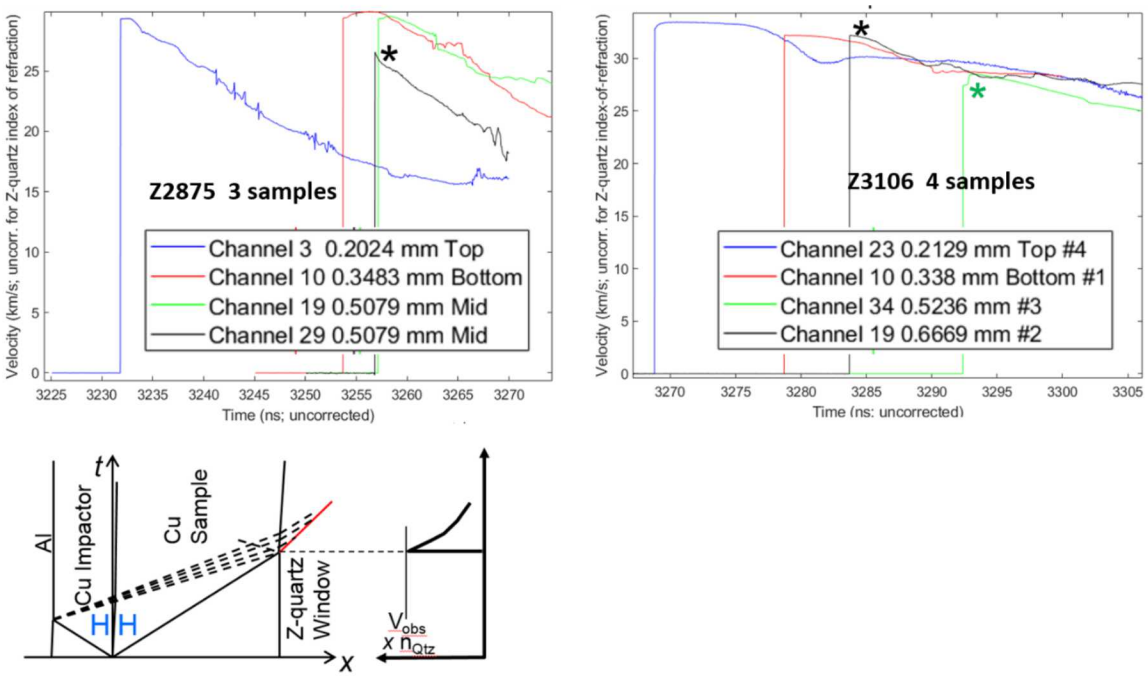

Figure 3.11. Waveform details from Z2875 and Z3106, showing potential rarefaction overtake situations. * = possible overtake. A wave-interaction drawing on the lower left shows an incipient overtake. Samples are numbered from bottom to top.

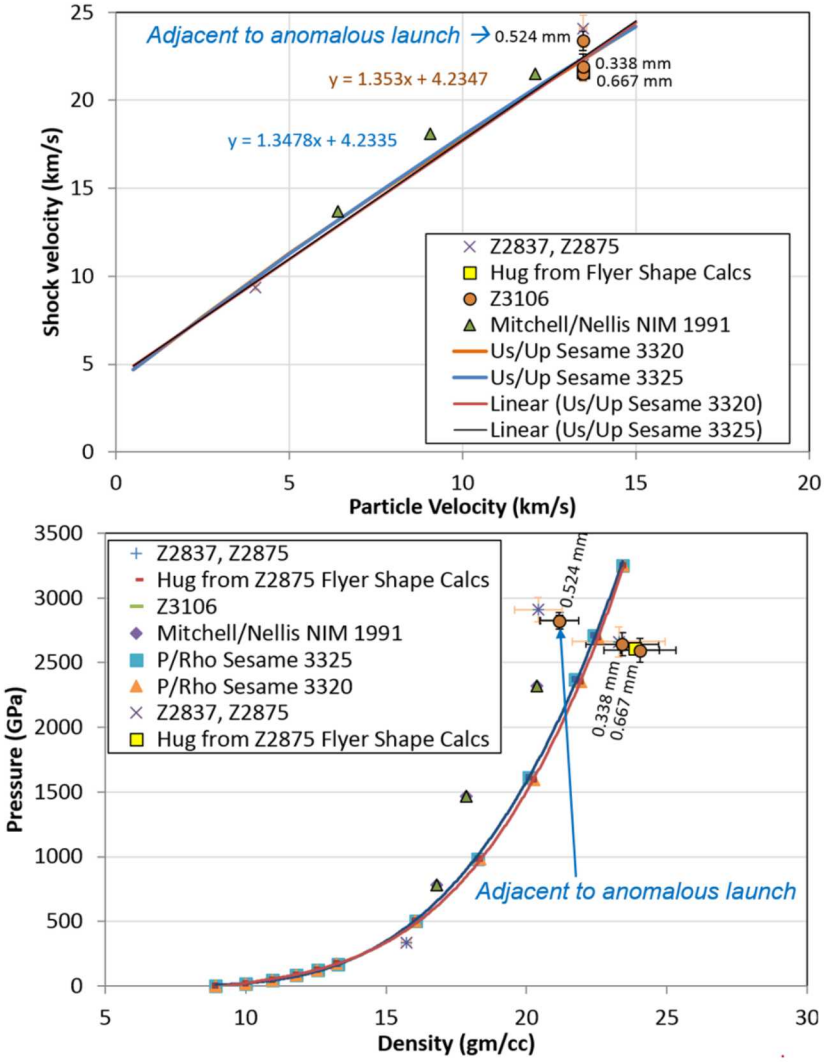

Figure 3.12. Hugoniot plots including Shot Z3106 results. The linear U_S-U_P relations are $C_0 = 4.2335$ and $S = 1.3478$ (Sesame 3325) and $C_0 = 4.2347$ and $S = 1.353$ (Sesame 3320).

3.4 Data Summary

The input data for these calculations are summarized in Table 3.1. The Hugoniot results are listed in Table 3.2. Due to the uncertainties in these, we have not attempted to extract the partial release states. A future researcher may yet extract sound speeds from the results of Z3106, but will have to bear in mind the uncertainties from (1) choosing release arrival points, and (2) the Hugoniot state.

Partial release states have been computed (and, by definition, lie on the z-cut α-quartz Hugoniot in pressure-particle velocity space); these are tabulated in Table 3.3. The impedance-match rationale is shown in Fig. 3.13. Strictly speaking, the last column in Table 3.3 (a sort of averaged release wave speed) is inaccurate because it is computed using steady-wave assumptions, and we do not expect those to apply here. However, it may offer a loose estimate of the sound speed at the Hugoniot.

Table 3.1. Input quantities for Hugoniot calculation

Test	Thickness mm	Impact Vel km/s	Impact Time μs	Breakout Time μs	ZQ Wavespeed mm/ μs
2837Mid	0.502(2)	8.06(4)	3.7472(5)	3.8008(5)	15.5(2)
2875Mid	0.497(2)	26.97(20)	3.2363(4)	3.2569(5)	46.8(5)
2875Bot	0.335(2)	26.97(20)	3.2386(4)	3.2539(5)	46.8(5)
3106MidTop	0.5236(10)	26.95(5)	3.6278(5)	3.65021(15)	46.8(2)
3106MidBot	0.6669(10)	26.95(3)	3.6305(5)	3.66154(15)	46.8(2)
3106Bot	0.338(1)	26.95(3)	3.6318(5)	3.64730(15)	46.8(2)

Table 3.2. Hugoniot states

Test	Pressure (GPa)	Particle velocity (mm/μs)	Shock Velocity (mm/μs)	Density (gm/cm^3)
2837Mid	338(5)	4.03(2)	9.4(1)	15.7(2)
2875Mid	2908(93)	13.48(10)	24.1(7)	20.4(8)
2875Bot	2664(114)	13.48(10)	22.0(9)	23.2(1.6)
3106MidTop	2823(67)	13.47(3)	23.4(6)	21.2(7)
3106MidBot	2596(44)	13.48(1)	21.5(4)	24.0(7)
3106Bot	2642(90)	13.47(2)	21.9(7)	23.4(1.3)

Table 3.3 Partial release states

Test	Up	P	Rho	Us
2837Mid	4.85(8)	129(4)	15.0(2)	16.3(2.1)
2875Mid	20.02(27)	1605(38)	12.2(7)	9.8(1.1)
2875Bot	20.02(27)	1605(38)	11.9(1.0)	7.0(1.1)
3106MidTop	20.02(11)	1605(15)	12.1(4)	8.8(0.6)
3106MidBot	20.02(11)	1605(15)	11.8(4)	6.3(0.4)
3106Bot	20.02(11)	1605(16)	11.9(4)	6.8(0.7)

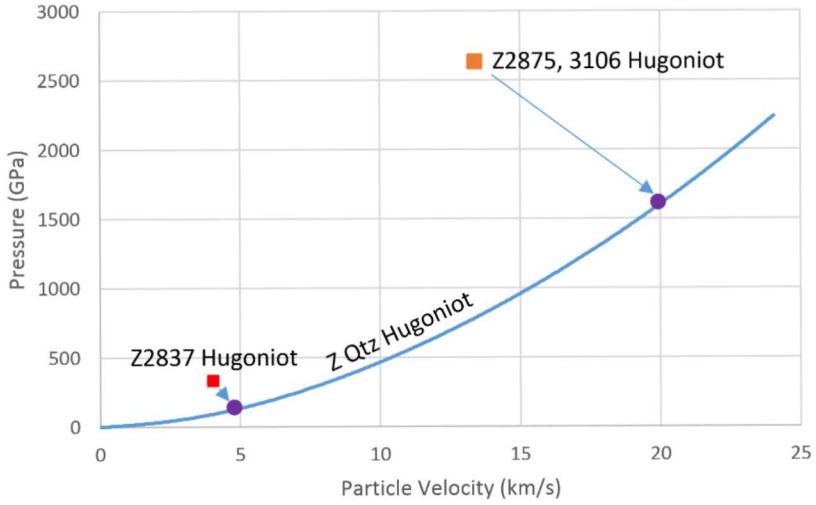

Figure 3.13. Partial release of Cu to Z-cut α-quartz window.

References

Barker, L.M. and Hollenbach, R.E., Laser interferometer for measuring high velocities of any reflecting surface, J. Appl. Phys., 43, 4669-4675, 1972.

Dolan, D. H. Foundations of VISAR analysis, Sandia National Laboratories report, SAND2006-1950.

Knudson, M. D. and Desjarlais, M.P., Shock compression of quartz to 1.6 TPa: Redefining a pressure standard, Phys. Rev. Lett. 103, 225501, 2009a.

Knudson, M. D. and Desjarlais, M.P., Adiabatic release measurements in α-quartz between 300 and 120 GPa: Characterization of α-quartz as a shock standard in the multimegabar regime, Phys. Rev. Lett. 103, 225501, 2009b.

Lemke, R.W., Knudson, M.D., Robinson, A.C., Haill, T.A., Struve, K.W., Asay, J.R and Melhorn, T.A., Self-consistent, two-dimensional, magnetohydrodynamic simulations of magnetically driven flyer plates, Phys. Plasmas, 10, 1867-1874, 2003.

Lemke, R.W., Knudson, M. D. and Davis, J.P., Magnetically driven hyper-velocity launch capability at the Sandia Z accelerator, Int. J. Impact Engrg, 38, 480-485, 2011.

Neogi, A. and Mitra, N, A metastable phase of shocked bulk single crystal copper: an atomistic simulation study, Scientific Reports, 7, 7337 (2017); doi:10.1038/s41598-017-07809-1

Distribution

Internal:

MS 1195	Dept. 1646	M. D. Furnish (electronic copy)
MS 1195	Dept. 1646	C. McCoy (electronic copy)
MS 0899	Dept., 9536	Technical Library (electronic copy)


Sandia National Laboratories